Desalination and Water Treatment
www.deswater.com

doi: 10.5004/dwt.2021.26731

213 (2021) 441–458
February

Activated carbon fiber from natural precursors: a review of preparation methods with experimental study on jute fiber

Md Raian Yousuf[a], Fatima Mahnaz[b], Sultana Razia Syeda[a,*]

[a]*Department of Chemical Engineering, Bangladesh University of Engineering and Technology, Dhaka-1000, Bangladesh, Tel. +880 1817 550666; email: syedasrazia @che.buet.ac.bd (S.R. Syeda), Tel. +880 1521 436045; email: raian.tanmoy@gmail.com (M.R. Yousuf)*
[b]*Department of Chemical Engineering, Bangladesh University of Engineering and Technology, Dhaka-1000, Bangladesh, Tel. +880 1744 244255; email: mahnaz.aishwariya@gmail.com*

Received 2 September 2019; Accepted 26 October 2020

ABSTRACT

Activated carbon fiber (ACF) has distinct advantages over other commercial porous storage materials in terms of capacity, kinetics and durability. Due to high processing cost of synthetic ACF, production of ACF from low-cost precursors, such as biomass or agricultural wastes, has drawn attention in recent times. In the first part of this study, a critical review of preparation methods of ACF based on ligno-cellulosic biomass and major factors affecting the key properties of the prepared ACF is presented. In the second part, an experimental study on jute fiber investigating chemical activation methods and properties of resultant ACFs are reported. Three key process parameters, that is, pretreatment method, activation temperature and concentration of activation agent were varied to get optimum result with respect to yield and adsorption capacity. Prepared ACFs were characterized by SEM and energy-dispersive X-ray spectroscopy analysis, iodine number and BET surface area test, and pore volume measurement. Additionally, adsorption isotherms, adsorption kinetics and adsorption capacities of the ACF for two organic dyes – methylene blue (MB) and 4-nitrophenol (4-NP), were investigated. The paper also describes the limitations of biomass-based ACFs and the challenges in commercializing them. Finally, scopes of further research to improve adsorption and mechanical properties as well as to meet the diversified market demand of biomass-based ACF are discussed.

Keywords: Activated carbon fiber; Jute fiber; Adsorption; Dye removal; Adsorption isotherm; Adsorption kinetics; Biomass

1. Introduction

The use of activated carbon for industrial applications started in the early 1900s [1]. A thermochemical approach including carbonization and activation was established for synthesizing activated carbon. The thermochemical method mainly transforms organic components of biological substances, such as wood, coal, coconut shells, etc., into chars. The activated carbon materials produced in this way are of particulate form and usually difficult to handle in many industrial systems. Additionally, due to certain disadvantages, such as slow kinetics, poor selectivity, low working capacity, etc., the application of active carbon materials have been somewhat limited.

The idea of activated carbon fiber (ACF) came into play to overcome some of the drawbacks of activated carbons mentioned above. ACFs are developed by carbonizing and activating carbonaceous fibers. These activated fibers have broader applications as they are easier to handle and they allow greater contact efficiency with the media leading to higher adsorption rate, higher surface area, better

* Corresponding author.

1944-3994/1944-3986 © 2021 Desalination Publications. All rights reserved.

durability and enhanced design flexibility compared with the particulate activated carbons [2]. Currently, ACFs are fabricated by the pyrolysis and activation of various organic fibers such as synthetic fibers, polyvinyl alcohol (PVA), polyaramide and phenolic resin, petroleum and coal-tar pitch fibers for commercial purposes. Thus, fossil fuels have been so far the most likely sources of the precursors for preparing ACFs commercially.

However, due to ever-increasing concerns on environmental pollutions and energy crisis fossil fuel is becoming less attractive as a feedstock [3,4]. On the other hand, biomass has become more promising as feedstock because of its abundance, environmental friendliness, low cost and good renewability [5]. Using natural fiber as precursor is particularly cost effective as it is naturally in fibrous shape and does not require expensive spinning step before carbonization and activation of the feedstock [6]. Besides, use of biomass as feedstock facilitates the tailoring of pore structures of ACFs [7–9]. Thus, there is a growing interest in using ligno-cellulosic materials such as jute, sisal, coconut, banana fibers, etc. as precursors for the production of ACFs [6,10–15].

The present study has focused on preparation of biomass-based ACF with two-fold objectives. First, a review of previous studies on synthesis of biomass-based ACF was carried out. The effects of different synthesis methods on the properties of ACFs were reviewed thoroughly. As ACF produced from natural fibers often have low yields, effects of oxidative stabilization, chemical pretreatment and chemical activation on yield were also investigated.

Additionally, an experimental work was undertaken to prepare ACF from locally available jute fiber. The adsorption isotherm, kinetics and dye removal capacities of the prepared ACFs had been studied. Jute was particularly used in the experiment due to the policy of Bangladesh government to promote technological and economic research on jute. Moreover, it is the second most common natural cellulose fiber worldwide and has excellent physical, chemical and structural properties. According to Bangladesh Jute Research Institute, a number of studies to explore the potential of jute in different applications such as knitting wool substitute; furnishing fabrics; preparing micro crystalline cellulose, jute felt, geotextile, charcoal from jute stick, etc. has been carried out in the past. There is, however, no study that investigated the potential of local jute fiber as a precursor for preparing ACF. It is imperative that local jute fiber is utilized to produce high capacity ACF to create possibility of extending its use in different applications, such as, absorbed natural gas (ANG) for LNG transport, wastewater treatment, removal of SO_2 and NOx from air, etc.

2. General methods of preparation of ACF

General protocol of ACF production follows a two-stage process of carbonization followed by activation of raw materials or precursors. Carbonization involves pyrolysis of the precursor in a non-oxidative atmosphere resulting in elimination of volatiles, loss of hydrogen, and a fixed carbon mass with a rudimentary porosity. The resulting low-porosity char is then activated, developing the porous network through an oxidation process.

2.1. Carbonization

In most cases, carbonization is performed by pyrolysis under a stream of an inert gas (typically nitrogen gas) at temperatures below 800°C, and leads to the elimination of the non-carbon species as volatiles during the thermal decomposition of the precursor, loss of hydrogen, and the formation of free radicals, which condense to form a rigid cross-linked solid char and a fixed carbon mass with a undeveloped pore structure [16]. It is a simultaneous process that changes both the chemical composition and physical phase of materials and is irreversible. The quality and yield of the carbonized material depend on the type and properties of the precursor, as well as carbonization parameters such as the rate of heating, the final temperature achieved, the retention time at this temperature and nitrogen flow rate [16]. While raising the temperature increases carbon content, it decreases the amount of volatile matter and the total mass giving lower yield. Again, too high temperature causes gasification of the mass. Therefore, ACF with greater quality is obtained by optimizing the temperature that would give sufficient yield as well as carbon content. Thus, a temperature range of 400°C and 850°C is usually used for carbonization process.

For synthetic fibers such as those prepared from PAN, pitch, resins, etc., carbonization provides the intermediate product, with high thermal and dimensional stability, and favorable chemical and biological resistance that subsequently goes for melting and spinning. Natural plant fibers can be directly carbonized without melting and spinning process, but with much lower yield. This excessive weight loss has been attributed to dehydration and chain-splitting reactions throughout the process [17]. This removes major non-carbon atoms from the atomic structure and leads to a carbon skeleton. Table 1 summarizes different stages of carbonization and their corresponding effect on the fiber [18].

The pores that are created during carbonization are very small and sometimes are blocked partially by disorganized carbon. Therefore, the pores in the carbonized material have to be further developed and enhanced by second thermal treatment process, known as activation process.

2.2. Activation

The specific surface area and porosity of carbons can be modified significantly by an activation process that removes the most reactive carbon atoms from the structure, thus increasing the surface area and porosity. During the activation step, the amorphous carbon produced in the initial carbonization step reacts with oxidizing gas in case of physical activation and with activation agent in case of chemical activation, forming new pores and opening closed pores. The process enhances the adsorptive capacity of the activated carbon. It needs relatively higher temperatures than carbonization for activation. Carbon activation procedures can be broadly divided into two main types: physical and chemical.

2.2.1. Physical activation

Physical activation is a heterogeneous, solid–gas reaction, involving the gasification of the more reactive portions of

the carbon skeleton of the carbonized precursor by oxidation with water vapor or carbon dioxide in the 850°C–1,000°C temperature range [16]. Physical activation develops porosity by the selective gasification of carbon with oxidizing gas at 850°C–1,000°C. The removal of carbon atoms creates pores, increases the average size of the micro-pores already accessible to the gas, and opens up closed pores that are created during carbonization. The most commonly used oxidizing gases are CO_2 and steam. They can be used either individually, as a mixture, or with an inert carrier gas. Carbon dioxide is usually used as activation gas as it is easy to handle, clean and possesses a slow reaction rate at a temperature around 800°C, which facilitates control of the activation process [19]. On the other hand, physical activation by steam is usually done at a temperature range of 500°C–700°C. The rate of reaction of carbon with steam is retarded by H_2 resulted from water–gas shift reaction taken place during activation [16].

2.2.2. Chemical activation

In the chemical activation process, carbonization and activation are carried out in a single step by the thermal decomposition of the precursor impregnated with chemical reagents. Chemicals that are widely used as activating agents are zinc chloride ($ZnCl_2$), potassium hydroxide (KOH), phosphoric acid (H_3PO_4), potassium carbonate (K_2CO_3), etc. These activating agents act as both dehydrating agents and oxidants so that carbonization and activation take place simultaneously [16]. The carbonized precursor is impregnated with the given chemical reagent in the form of a concentrated solution. The cellulosic content present in the sample gets broken down in this procedure. The impregnated material is then pyrolyzed again in the absence of air and under an inert environment, typically maintained by a stream of nitrogen gas. Chemical activation involves the reaction of the precursor with the activating agents at temperatures between 500°C and 800°C. In this stage, the chemical activator dehydrates the raw material, as a result of which the carbon skeleton is charred and aromatized, and a porous structure is created [16]. The product is then cooled and the chemical is removed by extensive washing with water and other suitable solvents, and this is followed by drying.

3. ACF prepared from natural fibers

Different natural fibers have been explored to produce ecofriendly and low-cost ACF. Emphasis is being placed on finding the right type of natural fiber and optimizing the preparation methods. The natural precursors widely reported in previous investigations are jute fiber, coconut fiber, bamboo fiber, waste cotton, etc. In following sections, preparation methods and properties of the synthesized ACFs from different natural fibers are summarized.

3.1. Jute fiber

Jute fiber has unique combination of physical, chemical and structural properties, and has been used to produce ACF in a number of studies due to its abundance [20,21]. The amount of carbon derivative components present in jute fiber is high and has the potential to be an effective precursor for ACF. Table 2 summarizes major components present in jute fiber in percentage [6,22].

Rombaldo et al. [20] investigated production methods and thermal degradation of ACFs produced from jute fiber. The authors used steam for carbonization and physical activation. The thermal analysis indicated that above 600°C there was no significant mass loss, as most of the volatile organic components were driven off. Table 3 presents the properties of ACFs found at different activation temperatures.

Rosas et al. [23] studied ACF from hemp fiber, which is similar to jute fiber with respect to fiber structure, carbon content and cellulosic content. The authors found 67.0% cellulose and 16.1% hemicellulose in the raw hemp fiber with 50.99% O and 43.17% C content. However, the ash content of the raw hemp fiber was considerably higher than that of raw jute fiber [6,23]. They prepared ACFs by both physical and chemical activation of hemp. Physical activation was carried out at temperature ranging from 450°C to 800°C under nitrogen flow. The chemical activation was carried out using 85% phosphoric acid with

Table 2
Major components of raw jute fiber

Component	Approximate percentage (%)
Cellulose	60
Hemicellulose	20
Lignin + pectin	15
C	45
O	45
H	7
N	0.10

Table 1
Mechanism of carbonization

Stage I (25°C–150°C)	Absorbed water is eliminated
Stage II (150°C–240°C)	Splitting up of the structural water occurs from hydrogen and hydroxyl fragments present. C=O and C=C bonds form, and the dehydration process is essentially intramolecular
Stage III (240°C–400°C)	Thermal degradation starts. Thermal cleavage of C–O and C–C linkage occurs
Stage IV (>400°C)	Each cellulose unit breaks down into a residue containing four carbon atoms, which then repolymerizes into carbon polymer and produces a structure by condensation reactions involving the removal of H_2

Table 3
Properties of ACF at different temperatures, prepared from jute fiber

Activation temperature (°C)	Activation time (min)	N_2 flow rate (mL/min)	Yield (%)	BET surface area (m^2/g)	Total pore volume (cm^3/g)
600	30	200	20.67	361.5	0.18
600	90	200	19.95	396	–
700	30	300	19.56	404.1	–
700	60	300	17.82	446	–
800	30	200	18.61	475.5	0.24
800	30	400	16.26	547.9	0.31
800	90	400	11.46	748	0.55

(–): not available.

impregnation ratio varying from 1 to 3 and temperature varying from 450°C to 550°C having a retention time of 2 h. Distilled water was used to wash the heat-treated fiber.

The study showed that the yield of the physically activated ACFs ranged from about 25% for a pyrolysis temperature of 450°C to about 12% for 800°C. It is worth noting that the yields of the chemically activated ACFs were almost twice the yields of the physically activated ACFs, that too with a significantly higher BET surface area and pore volume.

3.2. Coconut fiber

Coconut fiber is also reported to be used as a raw material for ACF preparation. Zhang et al. [5] used coconut fibers to produce ACF by chemical activation with KOH. The authors reported the morphology, composition, specific surface area, pore structure and thermal stability of the prepared ACFs. The specific surface area and pore volume of the prepared ACFs were reported to be 1,556 m^2/g and 0.72 cm^3/g, respectively.

Phan et al. [6] prepared ACFs from jute and coconut fiber. The authors used both physical and chemical activations for ACF production and compared the resultant properties. Physical activation consisted of a carbonization step at 950°C under nitrogen flow followed by an activation step with CO_2 flow at constant temperature.

In case of chemical activation, the raw fibers were impregnated with a solution of 30 wt.% H_3PO_4 and heated in an oven under nitrogen flow at 900°C. The fibers obtained were washed with deionized water and dried at 105°C. The diameters of the ACFs ranged between 50 μm and 10–20 μm. The SEM images showed that the macro-pores of activated coconut fibers were larger than those of activated jute fibers. BET surface area obtained for activated jute fiber varied from 912 to 960 m^2/g and for activated coconut fiber it varied from 1,088 to 1,303 m^2/g. A summary of processing parameters and key properties of the prepared ACFs in the two above-mentioned studies are given in Table 4.

3.3. Bamboo fiber

Bamboo fiber is reported to be a great precursor for low-cost ACF production. Zhao et al. [24] reported specific surface area up to 2,169 m^2/g for ACFs prepared from bamboo fiber. The authors used both carbonization and physical activation of bamboo fiber under nitrogen flow. They found that both mesopore and micropore volume increased with increasing activation temperature and retention time. A similar trend was observed for the BET surface area as well [24]. Hina et al. [25] reported preparation of bamboo-based ACFs through chemical activation by impregnating bamboo fibers with 200 g/L ammonium phosphate at a mass ratio of 1:10 (fiber:ammonium phosphate) for 24 h and heating the fibers at 200°C in air for 2 h. The pretreated samples were then heated from room temperature to 650°C. The surface area attained for activated bamboo fibers was 1,455.6 m^2/g.

3.4. Cotton

Both raw and waste cotton have been studied as precursors for ACF. Chiu and Ng [26] studied ACF prepared from cotton through chemical activation with $ZnCl_2$ in argon environment for removing methylene blue (MB) from water. The N_2 gas sorption analysis revealed that BET surface area and pore volume of the ACF to be as high as 2,060 m^2/g and 1.002 cm^3/g, respectively. Hina et al. [25] also reported ACFs prepared from cotton. The activation was carried out with ammonium phosphate at 650°C. The BET surface area attained was 1,020 m^2/g.

Ekrami et al. [27] reported effective use of waste textile fibers for production of ACF by thermochemical conversion. Aqueous H_3PO_4 was used with impregnation ratio varied from 0.5 to 3 for chemical activation of the waste cotton under continuous N_2 flow. The produced ACF was cooled and subsequently, washed with distilled water. The reported optimized conditions are activation temperature, 450°C; activation time, 0.5 h; impregnation ratio, 2 and heating rate, 10°C/min. The SEM photographs demonstrated broken fibers with wrinkled surface morphology and reduced diameter due to the severity of the activation conditions aided by the catalytic effect of phosphoric acid. However, the properties of the produced ACF reported in this study were found promising with iodine number, 1,018 mg I_2/g C; Langmuir specific surface area, 1,101 m^2/g; BET specific surface area, 694 m^2/g and micropore volume, 0.288 mL/g [27].

In a recent study, Silva et al. [28] reported production of ACFs from waste denim fabric consisting of 100% cotton

Table 4
Preparation conditions and properties of resultant ACFs from jute and coconut fibers

Source	Preparation condition							BET surface area (m^2/g)	Micropore volume (cm^3/g)
	Precursor	Carbonization temperature (°C)	Activation type	Activation temperature (°C)	N_2 flow rate (L/min)	Heating rate (°C/min)	Retention time (h)		
Phan et al. [6]	Jute	950	Physical (CO_2)	950	2.5	20	0.5	912	0.388
	Jute	–	Chemical (H_3PO_4)	900	2.5	20	2	959	0.381
	Coconut	950	Physical (CO_2)	950	2.5	20	0.5	1,088	0.473
	Coconut	–	Chemical (H_3PO_4)	900	2.5	20	2	1,303	0.536
Zhang et al. [5]	Coconut	600	Chemical (KOH activation)	900	0.03	10	2.5	1,556	0.49

(–): carbonization and activation occurs simultaneously in chemical activation.

for removing textile dyes from water. This study as well as other studies on dye removal by ACF indicates that adsorption of large molecules, for example, dye molecules, require the adsorbents to have a mesoporous structure [29,30]. This can be achieved by slow pyrolysis process and using acids, for example, H_3PO_4, as chemical activation agents.

Apart from the abovementioned natural precursors, limited studies on few other natural fibers such as pineapple plant leaves [29], sisal, flamboyant pods [31], vetiver roots [32], piassava fiber [33], kapok, ramie, viscose, lyocell [25], etc. show good potential of these fibers as ACF precursors.

4. Factors affecting properties of natural fiber–based ACF

In order to improve the quality and broaden the application of natural fiber–based ACFs, understanding of the factors affecting the properties of ACF is critical. In the following sections, the key factors and their effects on the properties of ACFs are summarized.

4.1. Temperature and residence time

In ACF production, the carbonization and activation temperature play a vital role in affecting the characteristics of the ACF produced. Low processing temperature may lead to low porosity and low fiber strength due to the volatile organic components that retain in the fiber. Again, increasing the temperature will enhance the surface area and porosity, however, may decrease the yield by gasification of carbon. Thus, optimal conditions for carbonization of precursor fibers are required to be defined and controlled. The conditions are optimized by changing the temperature and retention time. Ekrami et al. [27] reported activated waste cotton where activation temperature was varied between 350°C and 500°C, activation time between 0.5 and 4 h and temperature increase between 2°C and 10°C. The yield falls and iodine number increases with increasing temperature, activation time and temperature increase rate. The optimum conditions are as follows: activation time of 0.5 h, activation temperature of 450°C and the rate of temperature rise of 10°C/min.

4.2. Types of activation

Both physical and chemical activations are employed for biomass-based ACF. The temperature used for physical activation generally ranges from 800 to 1,100°C, whereas for chemical activation it is from 450°C to 900°C. The yield in case of physical activation is 10%–24%. On the other hand, the yield obtained in chemical activation is reported to be as high as 50%. The surface area attained for biomass-based ACFs varied from 450 to 1,600 m^2/g. It is also observed that the surface area and porosity of the ACFs obtained by chemical activation are similar to or higher than those obtained by physical activation. In addition, chemical activation results in active carbons with mixed pore structure, that is, micro-, meso-, macro-pores whereas physical activation leads to formation of predominantly micro-pores with diameter <2 nm and pore volume 0.6–0.8 cm^3/g [34–38]. Chemical activation is also reported to cause less damage to the carbon structure, and preserves the fiber integrity better

than physical activation. In addition, activation can also be carried out in a solution to create and modify functional groups and develop surface roughness (increase in surface area) of carbon fibers. This process is used for the modification of the pore chemistry of ACFs [34–38].

4.3. Types of chemical treatment of precursor.

The most reported reagents used for chemical activation of biomass are KOH, NaOH, $(NH_4)_2HPO_4$, $ZnCl_2$ and phosphoric acid. The reported impregnation ratio of chemical to carbonized fibers varies from 0.2 to 3 with $ZnCl_2$ and phosphoric acid; from 2 to 8 with KOH and NaOH and with $(NH_4)_2HPO_4$ the impregnation ratio reported is as high as 10 [39,40].

The impregnation ratio poses a great influence on the yield and porosity of the final carbon. It is reported that low impregnation ratio favors development of micro-porosity and higher concentrations of chemicals, that is, higher impregnation ratio helped in development of meso-porosity. It is also reported that the concentration range, in which micro-porosity is developed, is coupled with a high yield that decreases with higher concentration when meso-porosity is developed [39,40]. Furthermore, H_3PO_4 has been recommended over alkali hydroxides (KOH and NaOH) and $ZnCl_2$ for chemical activation as the latter are corrosive and can cause environmentally adverse effects [41].

Su et al. [42] and Su and Wang [43] indicated that pretreatment of cellulose fiber/fabrics with flame retardants, such as Lewis acids, bases, strong acids, halides, etc. can promote dehydration and reduce the amount of unfavorable levoglucosan that is produced in cellulosic fibers at higher temperature causing lower carbon yield and potential fire hazards. A number of studies reported pretreatment of precursors with flame retardants before heat treatment to improve the performance of physical activation. Ammonium sulfate and di-ammonium hydrogen phosphate are namely two-flame retardants that have been studied for pretreating cellulosic material [42,43]. The pretreatment is carried out by impregnating or spraying the fiber with flame retardants and then heating the fiber in N_2 or air at temperatures <400°C. Precursor pretreatment with flame retardants is reported to enhance dehydration, efficiency of carbonization and activation of cellulose, and increase carbon yield as well as improve fiber strength, pore structures, and adsorption properties of the resulting ACFs [39,40,43].

Duan et al. [44] prepared ACF from cotton via chemical activation assisted by microwave. The study reported highest surface area, and pore volume, 1,370 m^2/g and 0.98 cm^3/g, respectively, obtained at 640 W microwave with 10 min activation time and 50% H_3PO_4. The study also reported higher yield with microwave assisted activation than that with conventional furnace activation. Previously, Foo and Hameed [45] presented another study on microwave-assisted activation with KOH of oil palm fiber to produce ACF and reported somewhat similar result.

4.4. Type of washing

Most of the chemically activated fiber requires rigorous washing after heat treatment to remove impurities from the fiber pores. Washing in some cases involves additional chemicals such as HCl, ethanol, chloroform, etc. [42,46]. In most of the cases large amount of distilled/deionized water as high as 500 times of the resultant ACF is used for washing [5,6,27]. The washed fibers also require drying at a temperature around 104°C for 5–24 h at different stages of washing. Based on literature survey, Su et al. [42] reported that rinsing of chemically treated carbon fiber absorbents takes a significant amount of time, that is, about 74 h. The authors also suggested ultrasonic cleaning process requiring a washing time about 2 h as an alternative to traditional washing of chemically activated fiber.

5. Adsorption properties of natural fiber–based ACF

5.1. Adsorption isotherms

The classical Langmuir and Freundlich models, given below, are generally used to express the adsorption isotherms and to determine adsorption parameters of ACF.

The Langmuir isotherm assumes a surface with homogeneous binding sites, equivalent sorption energies and no interaction between adsorbed species. It is expressed as shown in Eq. (1):

$$\frac{c_e}{q_e} = \frac{c_e}{q_{\max}} + \frac{1}{q_{\max} K_L} \tag{1}$$

where q_e is the adsorption capacity at equilibrium (mg/g), c_e is the equilibrium concentration of solution (mg/L), and $q_{\max}$ (mg/g) and K_L (L/mg) are Langmuir constants related to adsorption capacity and affinity of adsorbate toward adsorbent, respectively, with $q_{\max}$ representing the maximum monolayer coverage of adsorbent with adsorbate and K_L representing the enthalpy of the adsorption [47].

The Freundlich isotherm is an empirical equation based on an exponential distribution of adsorption sites and energies. It is expressed as shown in Eq. (2):

$$\ln q_e = \ln K_f + \frac{1}{n} \ln c_e \tag{2}$$

where q_e is the adsorption capacity at equilibrium (mg/g), c_e is the equilibrium concentration of solution (mg/L), and K_f (mg/g)/(mg/L)$^{1/n}$ and n are Freundlich constants related to adsorption capacity and adsorption intensity, respectively. Here, K_f represents the relative adsorption capacity of the adsorbent and n represents the degree of dependence of adsorption on the c_e of the solution [47].

Phan et al. [6] reported both Langmuir and Freundlich isotherm parameters for phenol adsorption on coconut and jute fiber–based ACFs. The parameters indicated that the chemically activated fibers demonstrated a better adsorption performance compared with the physically activated ones. Activated coconut fiber showed higher BET surface area but lower phenol adsorption than those of the activated jute fiber. This apparent contradiction is attributed to the wider distribution of micro-pore size in activated jute fibers compared with that in activated coconut fibers. This result indicates that the adsorption mechanism in ACF is governed by both porosity and pore size distribution.

Al-Aoh et al. [48] studied adsorption of methylene blue (MB) on ACF prepared from coconut husk and compared

the results with the adsorption properties of commercial granular activated carbon (GAC). The study showed that both ACF and GAC adsorbed MB favorably following the trend of Langmuir isotherm. The ACF, however, showed much better adsorption performance than the commercial GAC, which may be attributed to higher surface area and meso-pores in ACF compared with those in GAC.

5.2. Kinetic models

Kinetic models are used to evaluate the performance and mechanism of adsorption on ACF. These models provide a measure of the adsorption uptake with respect to time at a constant pressure or concentration and are employed to measure the diffusion of adsorbate in the pores. Most commonly used kinetic models to evaluate ACF performance are pseudo-first-order, pseudo-second-order and intra-particle diffusion model presented below.

Pseudo-first-order linear model:

$$\ln\left(q_e - q_t\right) = \ln q_e - K_1 t \tag{3}$$

Pseudo-first-order non-linear model:

$$q_t = q_e\left(1 - e^{\left(-K_1 t\right)}\right) \tag{4}$$

where q_t (mg/g) is the adsorption capacity at time t (min), q_e (mg/g) is the equilibrium adsorption capacity, and K_1 (min^{-1}) is the rate constant of pseudo-first-order equation.

Pseudo-second-order linear model:

$$\frac{t}{q_t} = \frac{1}{K_2 q_e^2} + \frac{t}{q_e} \tag{5}$$

Pseudo-second-order non-linear model:

$$q_t = \frac{K_2 q_e^2 t}{1 + K_2 q_e t} \tag{6}$$

where K_2 (g/mg min) is the constant of pseudo-second-order equation.

Intra-particle diffusion model:

$$q_t = K_{\text{int}} t^{\frac{1}{2}} + C \tag{7}$$

where K_{int} is the intra-particle diffusion rate constant and C is the experimental constant.

Al-Aoh et al. [48] reported adsorption kinetics of methylene blue (MB) on activated coconut fibers. The authors analyzed adsorption kinetics by pseudo-first-order, pseudo-second-order and intra-particle diffusion kinetic models and found that the experimental data fitted the pseudo-second-order model best. Also, the regression coefficient (R^2) values for the intra-particle diffusion model was found to be relatively small demonstrating insignificant diffusion in the adsorption process of MB on the ACF [48].

Zhang et al. [5] prepared ACF using coconut palm fibers. They used methylene blue, Congo red and neutral red as model pollutants to study adsorption kinetics. The adsorption capacity and adsorption rate of MB were found to be the largest among the three. The observation was attributed to the small molecular size of MB that reduced the steric hindrance during adsorption process. The paper also analyzed adsorption kinetics by pseudo-first-order, pseudo-second-order and intra-particle diffusion kinetic models and found that data fitted the pseudo-second-order model best [5].

6. Experimental studies

Locally available jute fiber was used to prepare ACFs for the experimental studies. As discussed above the properties of ACF largely depend on parameters such as pretreatment process, carbonization and activation temperature, concentration of activating agent, retention time, etc. The experimental procedures were planned to determine the set of parameters that would provide best quality of ACF with respect to surface area and yield.

First, chemical activation was chosen as it provides better yield and fiber strength. The activation temperatures were varied from 550°C to 700°C with retention time varied from 30 min to 2 h depending on the activation temperature. Activating agents such as alkali hydroxides (KOH and NaOH) and $ZnCl_2$ were avoided due to their detrimental, corrosive, environmentally adverse effects, and limited reagent recovery efficiency [16]. Phosphoric acid (H_3PO_4) was chosen as it is free from harmful and unfriendly environmental effects. Two different concentrations of H_3PO_4 acid were used to study their effects on ACF properties. Also, two different methods of activation, that is, with and without chemical pretreatment were used for synthesis. Two different types of flame retardants, namely, dibasic ammonium phosphate (DAP) and a mixture of ammonium sulfate and DAP were used for pretreatment.

6.1. Raw material and chemicals

Jute fibers used to prepare ACF in this study were collected from Bangladesh Jute Research Institute (BJRI) in bulk. The jute fibers collected from BJRI had diameter in the range of 17–20 μm. The fibers were cleaned and cut into pieces of 5–6 cm length and 20 g of sample was weighed from the cut and cleaned jute fibers, for each experiment. Chemical reagents were of analytical grade and used as received without further purification. Sources of the reagents are listed in Table 5.

6.2. Proximate analysis of raw jute fiber

Three different parameters were measured under proximate analysis, namely moisture content, volatile organic compounds percentage and ash content using ASTM methods, that is, ASTM D2495-07 (2012), ASTM E872-82 (2006) and ASTM D1102-84 (2013), respectively.

6.3. Preparation of ACF

Two different ACF preparation methods were investigated in this work. In the first method, raw fiber was carbonized and subsequently, chemically activated with phosphoric

Table 5
List of chemicals used and their sources

Chemical used	Source	Location
Diammonium phosphate, 98% (w/w)	Merck Group	
Ammonium sulfate, 98.5% (w/w)	Merck Group	
Chloroform	Merck Group	G.A. Traders, 48/1, Purana Paltan, 3rd Floor Dhaka 1000, Bangladesh
Iodine	Merck Group	
Potassium iodide	Merck Group	
Phosphoric acid, 85% (w/w)	RCI Labscan	Dymon Science Park, 22/23 Delowar Complex 26, Shahid Nazrul Islam
Hydrochloric acid, 37% (w/w)	RCI Labscan	Sarak (Hatkhola), Dhaka 1203, Bangladesh
Methylene Blue (MB)	ACROS Organics	Janssen Pharmaceuticalaan 3a, 2440 Geel (Belgium), Acros Organics BVBA
4-Nitrophenol (4-NP)	ACROS Organics	(Authors collected the chemicals from the Department of Chemistry, BUET)

acid. In the second method, a modified protocol involving four major steps, that is, pretreatment with flame retardant, carbonization, chemical activation, and post-treatment by chemical rinsing was followed.

6.3.1. Preparation of ACF without chemical pretreatment

Raw jute fiber was washed with distilled water and dried to remove any impurities present in the fiber. The fiber was then carbonized in a Nabertherm GmbH L5/12/P330 muffle furnace at 550°C for an hour with 0.15 L/min of nitrogen flow inside the furnace to maintain an inert environment. The sample was then cooled to room temperature and washed with 0.1 N HCl to remove impurities and dried. For chemical activation, the carbonized fiber was soaked in 35% H_3PO_4 for 24 h and subsequently heated at an activation temperature of 550°C for 2 h under 0.15 L/min nitrogen flow. The ACF was then cooled to room temperature and washed with distilled water and dried for further use. The same procedure was followed for chemical activation at 650°C, with a retention time of 1.5 h and nitrogen flow of 0.2 L/min.

6.3.2. Preparation of ACF with chemical pretreatment

In this method, two different types of flame retardants, 12.8% DAP and a mixture of 25.5% ammonium sulfate, and DAP having a weight ratio of 95:5 were used for pretreatment of the jute fiber as suggested by Su and Wang [43] and Su et al. [42]. Twenty grams of jute fiber was soaked for 24 h in the flame retardants for the pretreatment of each sample. The soaked samples were heated in the muffle furnace for carbonization at 550°C for about an hour with 0.15 L/min of nitrogen flow. The samples were then cooled to room temperature and washed with 0.1 N HCl to remove impurities. The washed samples were filtered with distilled water and oven dried for about 3 h.

Pretreated and carbonized samples were then impregnated with 50 mL solution of H_3PO_4 for 24 h. In this study, two concentrations of H_3PO_4, 35% (w/w) and 65% (w/w), were used. The impregnated samples were then heated in a muffle furnace under continuous nitrogen flow. In this study, four different temperatures, that is, 550°C, 600°C, 650°C and 700°C were used for activation. While operating at 550°C and 600°C nitrogen flow rate was kept at 0.15 L/min and samples were heated for 2 h, while at 650°C nitrogen flow rate was kept at 0.2 L/min and samples were heated for about 1.5 h. The activation temperature was increased to 700°C, with nitrogen flow rate of 0.8 L/min and samples heated for 30 min.

The activated samples were subjected to a series of chemical rinsing. First, the samples were kept in boiling 1 N HCl for an hour inside a fume hood to remove impurities followed by a rinsing with distilled water in a Soxhlet apparatus to remove excess chloride ions. The samples were subsequently desiccated in a stove at 104°C for 5 h followed by another rinsing with ethanol for 5 h in the Soxhlet apparatus and dried. The dried samples were washed with chloroform for 5 h in the same apparatus. Finally, the product was washed with distilled water for 5 h to remove excess acid, while it remained in the Soxhlet apparatus followed by drying and cooling of the samples to room temperature inside a desiccator.

6.4. Characterization

In this study, external and accessible internal pore surfaces of the ACF were measured by Micromeritics, PulseChemiSorb 2705 machine using three different concentrations of nitrogen gas namely, 15%, 30% and 50%. Samples were degassed at 250°C for 120 min before analyses. Iodine number was measured by a three-point adsorption isotherm following the ASTM D4607-94 (2011) method. SEM images of raw jute fiber and prepared ACFs were captured to visualize and compare pore structures. SEM and energy-dispersive X-ray spectroscopy (EDS) analyses were carried out using JEOL JSM-7600F at the Department of Glass and Ceramic Engineering, BUET. All the samples were dried at 200°C in vacuum for 180 min prior to analyses.

6.5. Adsorption isotherm

Adsorption isotherms of the prepared ACFs were studied using dye solutions of methylene blue (MB) and 4-nitrophenol (4-NP). A series of MB and 4-NP aqueous solutions were prepared with different concentrations to determine the concentration vs. absorbance curve of each dye in the corresponding maximum wavelength for calibration. The ACF prepared from pretreated jute fiber with DAP and activated with 35% H_3PO_4 at 700°C for 30 min was chosen for adsorption study.

Typically, 25 mg of ACF was added to 50 mL of dye solutions maintained at a fixed pH (pH = 8) in an orbital shaker shaking at 120 rpm for 24 h. The maximum absorption wavelengths of methylene blue and 4-nitrophenol aqueous solution were found at 667 and 301 nm, respectively. Six different initial concentrations, that is, 20, 60, 80, 100, 150 and 200 ppm of dye solution were used for the experiment.

The change in residual dye concentration was monitored using a SHIMADZU UV-1800 UV visible spectrophotometer. The adsorption capacity (q_e) was calculated using Eq. (6):

$$q_e = \left(c_0 - c_e\right) \times \frac{V}{m} \tag{8}$$

where c_0 (mg/L) is the initial concentration of dye solution, c_e (mg/L) is the residual concentration of dye solution, V (L) is the volume of dye solution, and m (g) is the mass of ACF used. The variation of residual dye concentration was monitored with respect to time.

7. Results and discussion

The characterization of raw jute fiber and produced ACFs, and adsorption properties of the produced ACFs are presented and discussed in the following sections:

7.1. Proximate analysis

The proximate analysis of cleaned jute fibers used in this study and those obtained from literature are presented in Table 6.

7.2. BET surface area and yield

The yield of jute fiber after activation was studied against pretreatment methods and two process parameters, that is, temperature of activation and concentration of chemical activation agent, H_3PO_4. Fig. 1a shows the trend of yield with increasing activation temperature at different

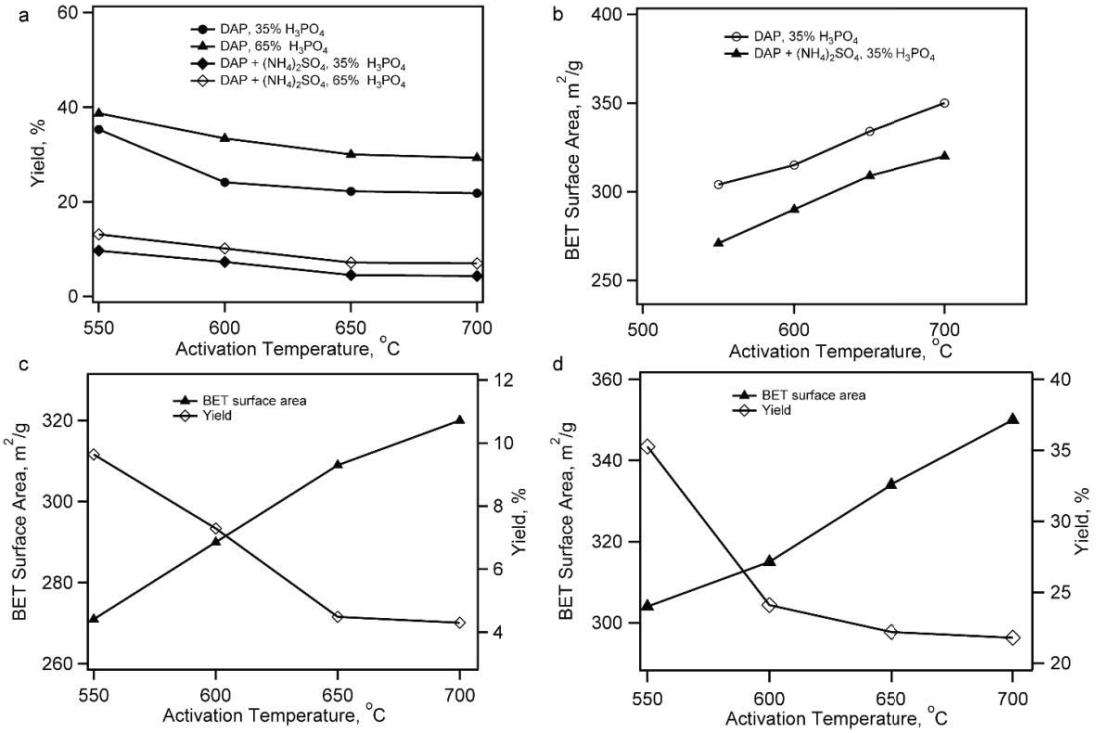

Fig. 1. (a) Plot of yield vs. activation temperature with respect to pretreatment method and H_3PO_4 concentration. (b) Plot of BET surface area vs. activation temperature with respect to pretreatment method at constant H_3PO_4 concentration. (c) Plot of BET surface area and yield with respect to activation temperature for DAP and ammonium sulfate pretreated sample, activated with 35% H_3PO_4. (d) Plot of BET surface area and yield with respect to activation temperature for DAP pretreated sample, activated with 35% H_3PO_4.

Table 6
Results of proximate analysis of raw jute fiber

Sample	Analysis	Present study, %	Literature, %
Raw jute fiber	Moisture content	8.7	10–12
	Ash content	0.4 (dry basis)	≈0.6 (dry basis)
	Volatile organic compounds	0.7	–

(–): not available.

pretreatment methods and H_3PO_4 concentrations. DAP-treated samples gave higher yields than the DAP and ammonium sulfate mixture treated samples. Also, higher H_3PO_4 concentration gave greater yields for both types of pretreatments.

Fig. 1b shows the effect of activation temperature on BET surface area for the two pretreatment methods. The figure shows that increasing activation temperature increases the BET surface area and DAP-treated ACFs give better results than those of the mixture-treated ones.

The trade-off between BET surface area and yield with respect to activation temperatures are shown in Figs. 1c and d for the two pretreatment methods. The yield decreased slightly between 650°C and 700°C with appreciable increase in BET surface area in both cases.

Table 7 summarizes yield, BET surface area and pore volume of ACF samples with respect to different preparation conditions. The highest yield (~40%) was obtained for the DAP-treated sample activated with 65% H_3PO_4 at 550°C for 2 h. The highest BET surface area, that is, 552 m^2/g, on the other hand, was obtained with DAP-treated sample, activated with 65% H_3PO_4 at 700°C for 30 min, with a yield of 29.3%.

At higher activation temperatures, retention time had to be set lower to prevent burning of the sample and to attain appreciable yield. The optimum retention times are presented in Table 7 along with other preparation parameters. The table also shows that the higher concentration of activating agent, that is, H_3PO_4 gave greater yield and larger BET surface area. It is noteworthy that the sample prepared at activation temperature 550°C without pretreatment gave significantly lower yield, BET surface area and pore volume than those of the pretreated samples prepared using similar method.

7.3. Surface morphology – SEM analysis

Fig. 2a shows surface morphology of raw jute fiber in fibrous shape. Fig. 2b shows carbonized jute fiber at 550°C with few visible pores in the fiber. Fig. 2c shows ACF sample prepared by chemical activation of raw jute fiber with 35% H_3PO_4 at 550°C. In this image, increased number of pores in the fiber resulted from chemical activation is evident. Fig. 2d shows the surface morphology of ACF prepared by chemical activation of raw jute fiber with 35% H_3PO_4 at 650°C. Pieces of broken fibers are visible in this image. Figs. 2c and d demonstrate the importance of activation temperature in sustaining the fibrous shape of ACF.

Figs. 2e and f show images of ACF pretreated with mixture of DAP and ammonium sulfate, and with DAP, respectively, keeping all other conditions same as those for the sample shown in Fig. 2d including the activation temperature 650°C. These images demonstrate that pretreatment of ACF contributed significantly in maintaining fibrous shape of the precursor at a higher activation temperature. The diameters of the ACF samples measured from SEM were between 14 and 16 μm while the lengths of the ACFs were in the range of 4–5 cm. These last two images also show that DAP-treated fiber exhibits better pore structure than the mixture treated one.

7.4. Elemental analysis by energy-dispersive X-ray spectroscopy

In order to detect the changes in the elemental components, EDS spectra of jute fiber before and after carbonization, and after chemical activation were analyzed.

Fig. 3a shows the EDS pattern of raw fiber indicates the peaks at 0.277, 0.392, 0.525 keV for corresponding K cell of carbon, nitrogen and oxygen belonging to the cellulose, lignocellulose and lignin components of jute fiber. The inset table shows mass and atom percentage of the elements. It is evident from the table that there is substantial amount of elemental carbon present in raw jute fiber that can be utilized for ACF production. EDS of carbonized fiber (Fig. 3b) shows an increase in carbon percentage due to the pyrolysis of volatile organic components.

Table 7
Yield, BET surface area and pore volume with respect to preparation conditions

Preparation condition of ACF	Concentration of H_3PO_4 (%)	Yield (%)	BET surface area, S_{BET} (m^2/g)	Pore volume, (cm^3/g)
No pretreatment, activated at 550°C for 2 h	35	6.9	190	0.1213
DAP treated, activated at 550°C for 2 h	35	35.27	304	0.23375
	65	38.9	353	0.24015
DAP plus ammonium sulfate treated, activated at 550°C for 2 h	35	9.64	271	0.21533
DAP treated, activated at 600°C for 2 h	35	24.1	315	0.23535
DAP plus ammonium sulfate treated, activated at 600°C for 2 h	35	7.29	290	0.21744
DAP treated, activated at 650°C for 1.5 h	35	22.2	334	0.23683
	65	30.0	516	0.39853
DAP plus ammonium sulfate treated, activated at 650°C for 1.5 h	35	4.49	309	0.21938
	65	7.15	447	0.22575
DAP treated, activated at 700°C for 30 min	35	21.8	350	0.23856
	65	29.3	552	0.42157
DAP plus ammonium sulfate treated, activated at 700°C for 30 min	35	6.3	320	0.22415
	65	6.98	460	0.23215

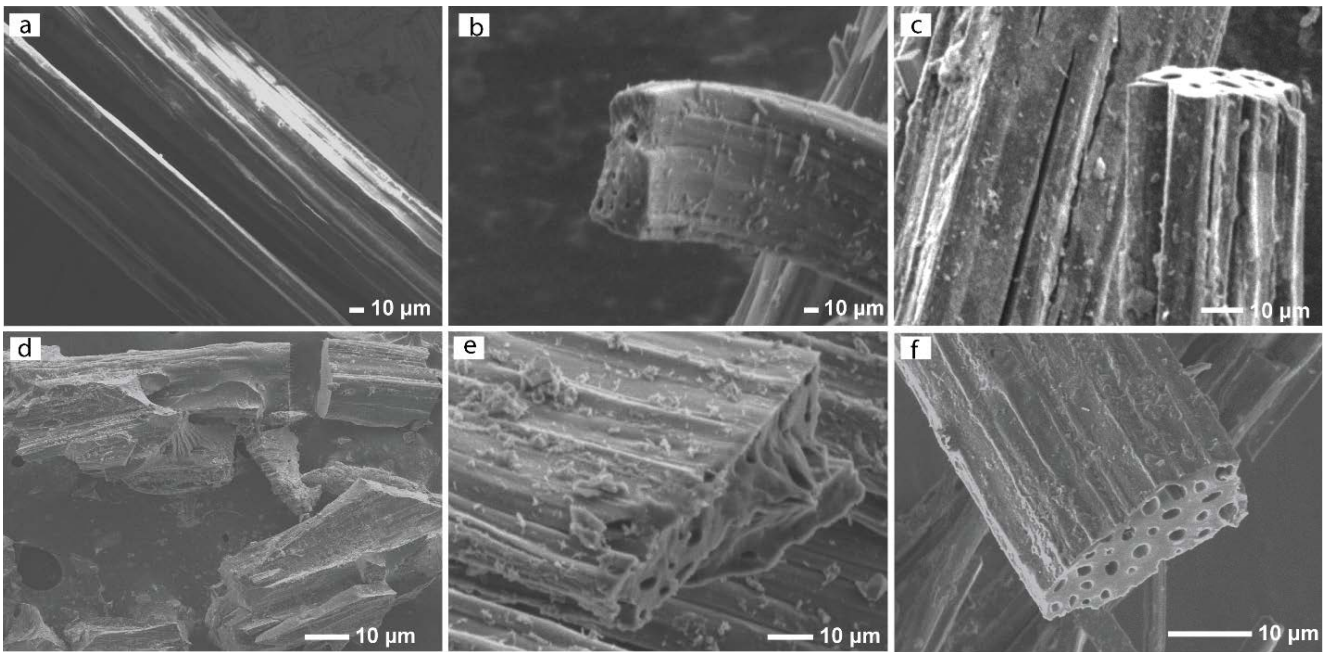

Fig. 2. SEM image of (a) raw jute fiber, (b) carbonized jute fiber at carbonization temperature 500°C, (c) ACF without pretreatment, activated with 35% H_3PO_4 at 550°C, (d) ACF without pretreatment, activated with 35% H_3PO_4 at 650°C, (e) ACF pretreated with DAP and ammonium sulfate, activated with 35% H_3PO_4 at 650°C, (f) ACF pretreated with DAP, activated with 35% H_3PO_4 at 650°C.

The carbonized jute fiber still retained high levels of oxygen and nitrogen because the raw material itself contained these two elements. Carbon percentage further increased after activation as shown in Fig. 3c. The inset table shows that nitrogen and oxygen reduced in this step. The reduction in oxygen may be due to the partial decomposition of oxygen by secondary high-temperature treatment during activation [5]. Also, small amount of phosphorus is present in the sample due to chemical activation using H_3PO_4.

7.5. Iodine number test

The amount of iodine absorbed (in milligrams) by 1 g of carbonaceous sample under specific conditions is called the iodine number. The iodine number is a relative indicator of porosity in an activated carbon material. It varies with changes in carbon in raw materials, processing conditions, and pore volume distribution. Presence of adsorbed volatiles, sulfur and water extractable may affect the iodine numbers.

The iodine numbers along with Freundlich isotherm parameters obtained for different ACF samples are presented in Table 8. It is evident from the table that the Iodine number increases with increasing activation temperature. This increase is more pronounced for DAP-treated samples than DAP and ammonium sulfate mixture treated samples.

7.6. Study on adsorption isotherm

Adsorption isotherms of the ACFs were generated using two organic dye pollutants, methylene blue (MB) and 4-nitrophenol (4-NP). The dye adsorption capacity of ACF is plotted with respect to initial concentration of solution in Fig. 4. The figure shows that the adsorption

Table 8
Iodine number and relevant adsorption parameters for the prepared ACFs

Preparation condition of ACF	Activation temperature, °C	Iodine number, X/M (mg/g)	Freundlich constant, K_f(mg/g)/(mg/L)$^{1/n}$	1/n	Correlation coefficient, R^2
DAP treated, chemically activated with 35% H_3PO_4	550	718	2,691	0.3378	0.9789
	600	720	14,725	0.7714	0.9999
	650	763	11,883	0.702	0.9902
	700	862	21,850	0.8263	0.9709
DAP plus ammonium sulfate treated, chemically activated with 35% H_3PO_4	550	698	5,546	0.5297	0.8885
	600	706	8,442	0.6344	0.9053
	650	724	3,312	0.3888	0.9982
	700	748	2,205	0.2909	0.9831

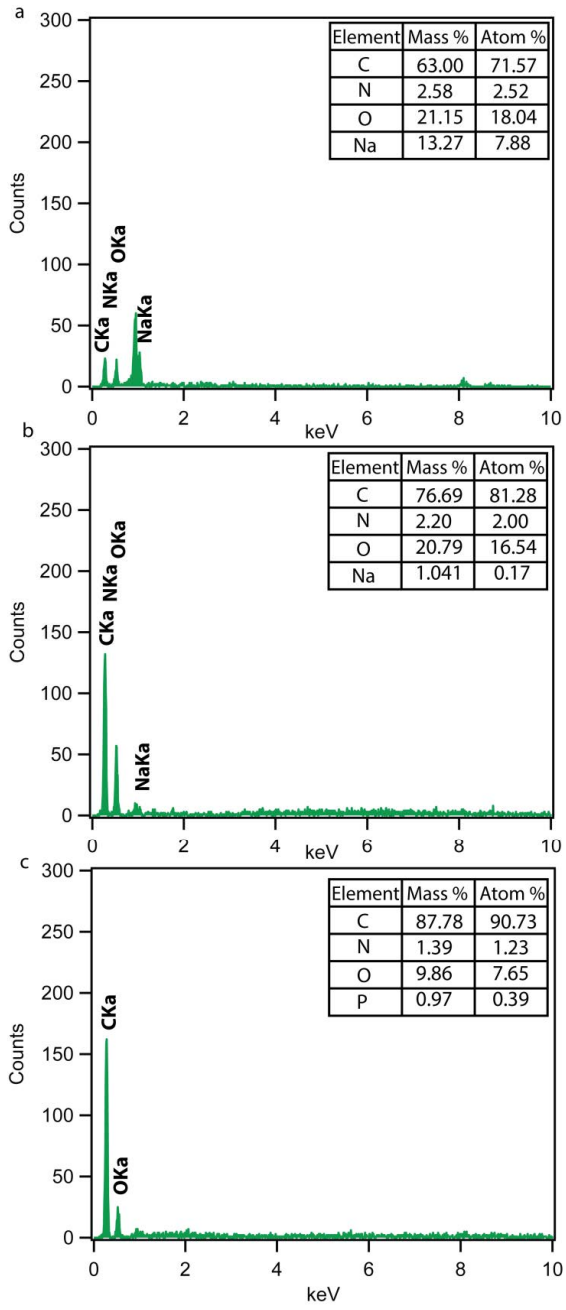

Fig. 3. Energy-dispersive X-ray spectroscopy analysis of (a) raw jute fiber, (b) carbonized jute fiber at 500°C, (c) ACF pretreated with DAP, activated with 35% H_3PO_4 at 700°C after chemical rinsing.

capacity for 4-NP is higher than that for MB. The higher molecular weight of MB creating larger steric hindrance during adsorption process may lead to this phenomenon.

Equilibrium data for MB and 4-NP adsorption onto ACF samples were fitted against the two most commonly used isotherm models namely, Freundlich and Langmuir isotherms, shown in Fig. 5. The parameters of the two models and the co-efficient of determination (R^2) were determined by linear regression and listed in Table 9. The table

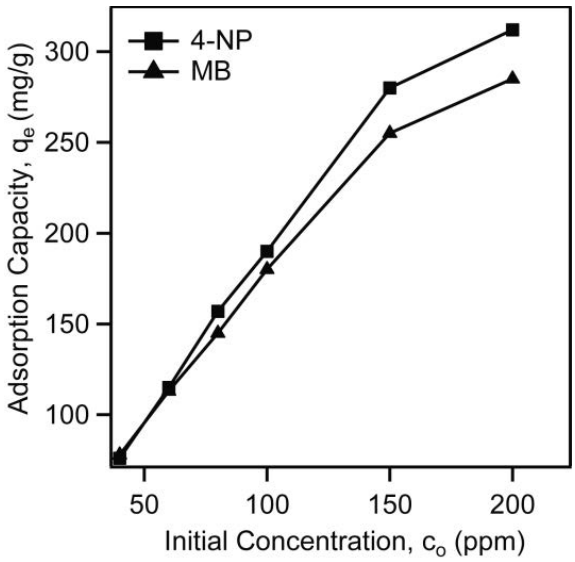

Fig. 4. Effect of initial concentration of dye solution on adsorption capacity.

shows that for both types of dyes, R^2 values are higher for Langmuir isotherm than those for Freundlich isotherm indicating a better fit of Langmuir model between the two models investigated. This also suggests that the solutes are possibly adsorbed in monolayer on ACF surface [48]. For MB, this result is consistent with other previous studies [26,30,44–46,48]. The monolayer adsorption capacities (q_{max}) for MB and 4-NP were found to be 312.5 and 322.58 mg/g, respectively, indicating decent values for maximum monolayer coverage. On the other hand, the $1/n$ value of Freundlich isotherm is in the range of 0.1 to 0.5 for both dyes, which indicates that the dye molecules are favorably and easily adsorbed on ACF surface from the solution [46,48].

7.7. Study on adsorption kinetics

Adsorption kinetics of ACF was determined with a fixed initial concentration of 20 ppm. The change of concentration of dyes in solution due to adsorption was noted with time. Fig. 6 shows the plot of adsorption capacity (q_e) vs. time. It is observed that the adsorption capacity increased rapidly in the first 20 min and then flattened gradually as the ACF approached its saturation point. The adsorption of MB and 4-NP reached equilibrium after 80 and 85 min, respectively. Fig. 6 also suggests that the adsorption rate of 4-NP was somewhat higher than that of MB. The early adsorption rate was faster as there were plenty of active sites for adsorption and the concentration gradient was higher. As the dye molecules started getting adsorbed, the number of active sites decreased and the concentration gradient dropped resulting in decline of the adsorption capacity. Also, the effect of steric hindrance decreased the rate of adsorption of the dyes.

A kinetic model is used to evaluate the performance and mechanism of adsorption of ACF. Most commonly used kinetic models to evaluate ACF performance are

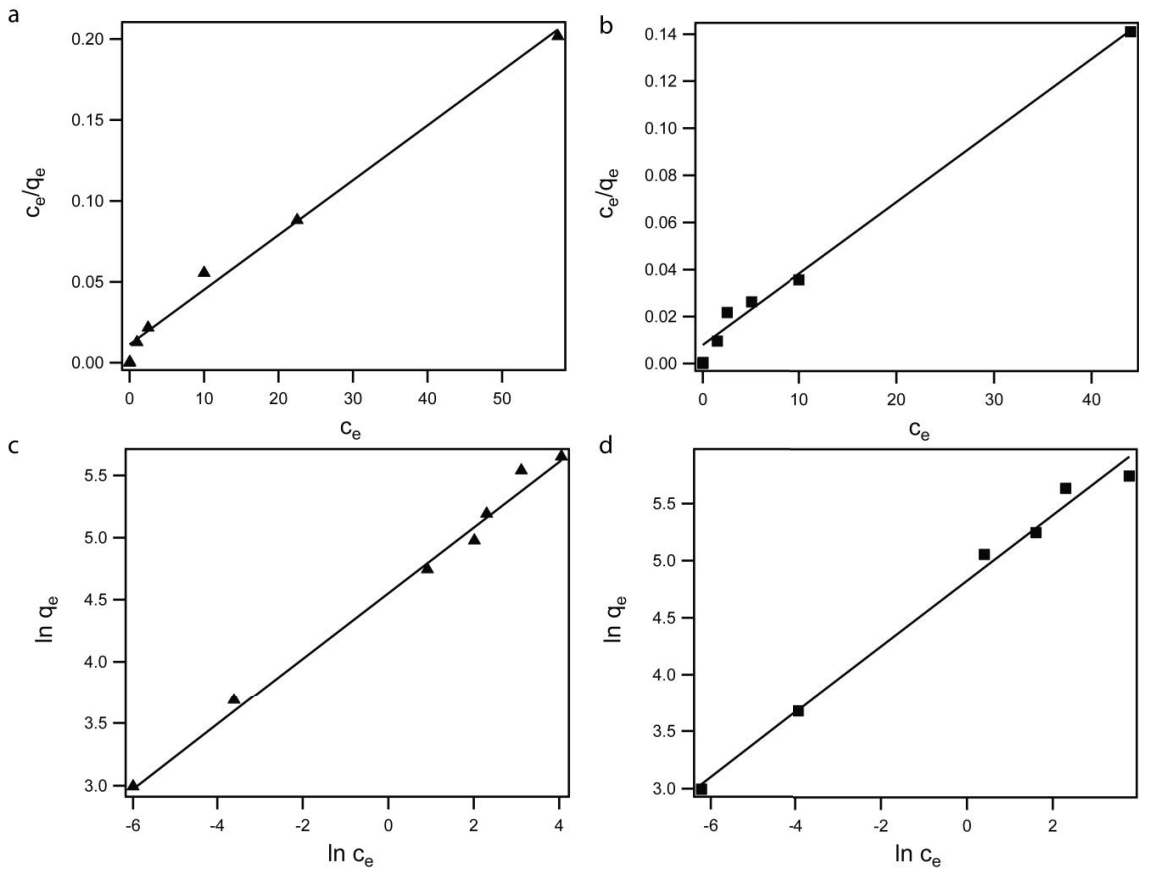

Fig. 5. Model fit for different isotherms: (a) Langmuir model for MB, (b) Langmuir model for 4-NP, (c) Freundlich model for MB, and (d) Freundlich model for 4-NP.

Table 9
Parameters of Freundlich and Langmuir isotherm models

Dye	Freundlich model			Langmuir model		
	$1/n$	K_f (mg/g)/(mg/L)$^{1/n}$	R^2	q_{max} (mg/g)	K_L (L/mg)	R^2
4-NP	0.280	115.58	0.904	322.58	0.516	0.982
MB	0.488	47.99	0.985	312.5	0.180	0.991

pseudo-first-order (PFO), pseudo-second-order (PSO) and intra-particle diffusion models. The adsorption kinetics of MB and 4-NP on ACF was studied using the adsorption equilibrium data.

Figs. 7a and d present the linear fitting of the PFO kinetic equation in $\ln(q_e - q_t)$ vs. t plot. Figs. 7b and e give the linear fitting of PSO kinetic equation in t/q_t vs. t plot. Finally, Figs. 7c and f shows the intra-particle diffusion equation fitted in the plot of q_t vs. $t^{1/2}$. Here, t denotes adsorption time in minutes.

The calculated kinetic parameters based on Eqs. (3), (5) and (7) and the plots presented in Fig. 7 are summarized in Table 10.

The equilibrium adsorption capacities (q_e) of MB and 4-NP measured in the kinetic experiment were 39 and 39.9 mg/g, respectively. However, the values of q_e for MB and 4-NP calculated through linear regression of PFO model, as can be seen from Table 10, are far below the measured values. Accordingly, non-linear regression of the PFO model

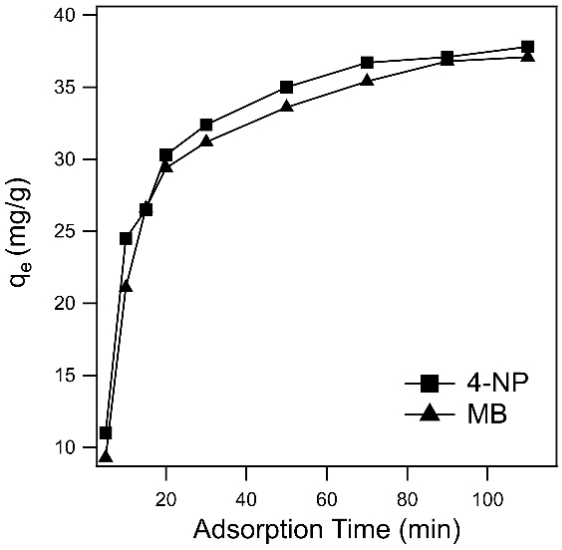

Fig. 6. Effect of adsorption time on the adsorption capacity.

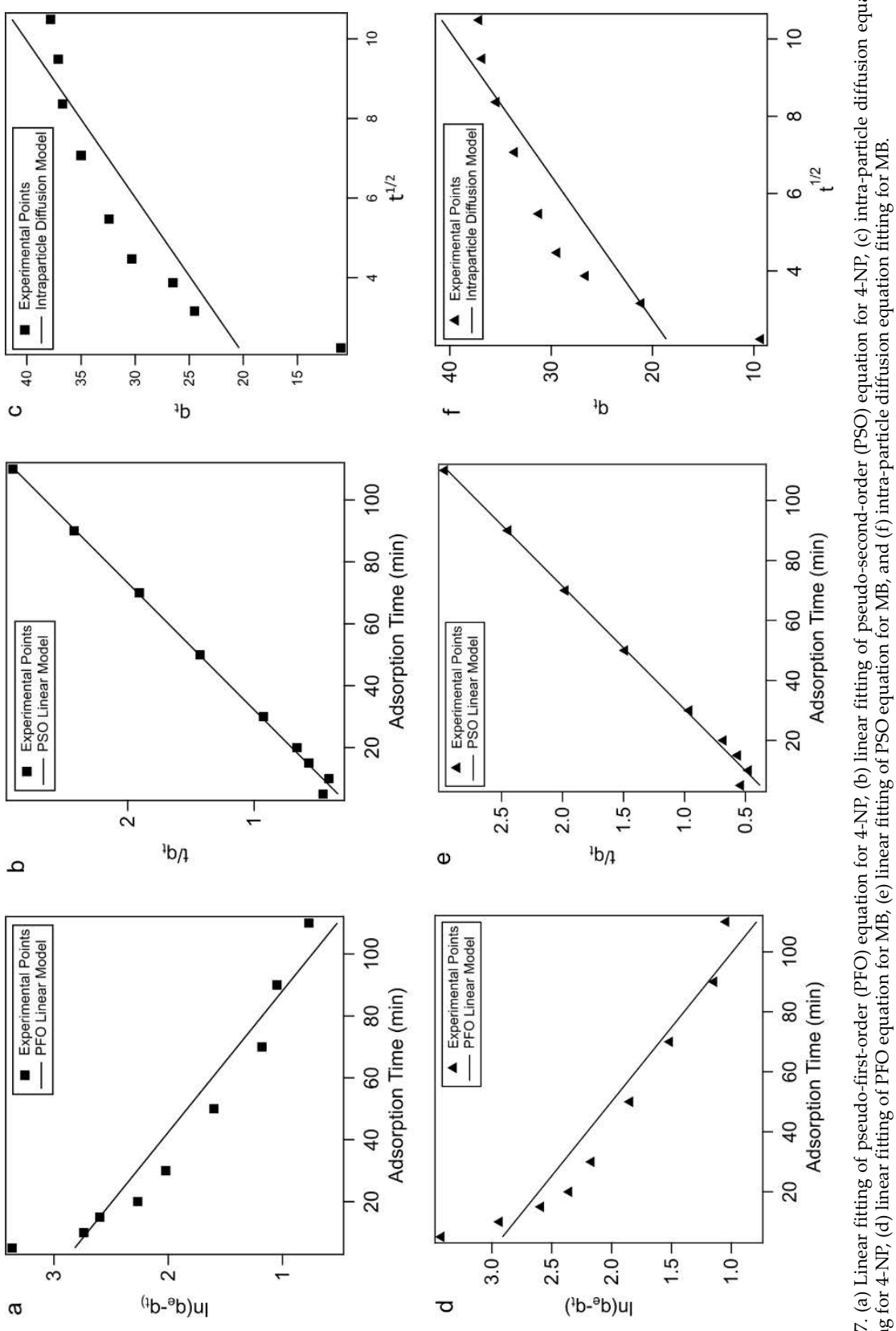

Fig. 7. (a) Linear fitting of pseudo-first-order (PFO) equation for 4-NP, (b) linear fitting of pseudo-second-order (PSO) equation for 4-NP, (c) intra-particle diffusion equation fitting for 4-NP, (d) linear fitting of PFO equation for MB, (e) linear fitting of PSO equation for MB, and (f) intra-particle diffusion equation fitting for MB.

Table 10
Kinetic parameters of different kinetic adsorption models obtained through linear regression

Dye	PFO model			PSO model			Intra-particle diffusion model		
	K_1	q_e	R^2	K_2	q_e	R^2	K_{int}	R^2	Intercept
4-NP	0.021	18.6	0.904	0.0028	41.0	0.9971	2.542	0.748	14.716
MB	0.020	20.31	0.901	0.0023	40.9	0.9949	2.686	0.759	12.64

PFO: pseudo-first-order; PSO: pseudo-second-order.

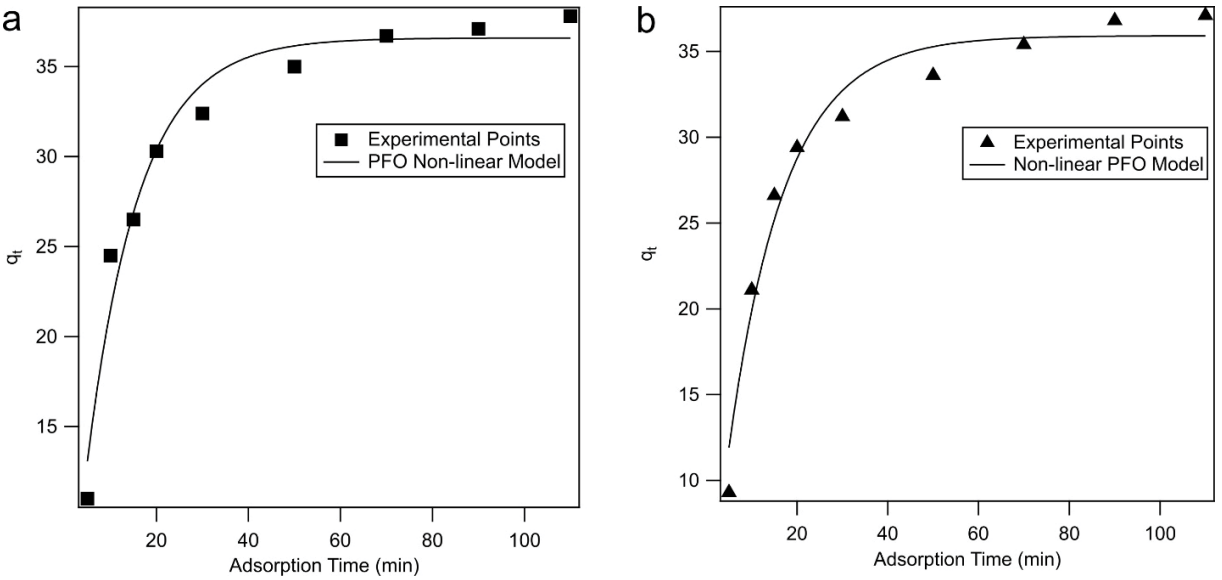

Fig. 8. (a) Non-linear fitting of pseudo-first-order (PFO) equation for 4-NP and (b) non-linear fitting of PFO equation for MB.

was carried out by plotting q_t vs. adsorption time (t), and fitting against Eq. (4). Fig. 8 presents the non-linear fitting of the PFO model for both 4-NP and MB. The corresponding calculated kinetic parameters are presented in Table 11.

Tables 10 and 11 show that, under the same adsorption conditions, the PSO kinetic model exhibits the best fit and describes the dynamic adsorption process of MB and 4-NP on ACF more accurately than the rest two models. The corresponding PSO kinetic equations are $\frac{t}{q_t} = 0.2593 + \frac{t}{40.9}$ for MB and $\frac{t}{q_t} = 0.2146 + \frac{t}{41}$ for 4-NP. These results are consistent with earlier studies on adsorption of MB by ACF [5,26,30,44–46,48]. Furthermore, adsorption capacities (q_e) calculated through non-linear regression of the PFO model agree better with the experimental values and exhibit better fit than those calculated through linear regression.

Table 12 summarizes the experimental and calculated capacities of 4-NP and MB adsorption on the ACF in both mass and molar basis. Although the mass capacities are similar for both dyes, more molecules of 4-NP were adsorbed on ACF compared with the molecules of MB.

Adsorption mechanism was investigated using the plot of Weber and Morris intra-particle diffusion model. As shown in Figs. 7c and f, the experimental data fit is poor for this model. Thus, it may be concluded that the intra-particle diffusion of dye molecules on ACF is not the rate controlling step in MB and 4-NP adsorption process. This is also consistent with the previous studies [5,44,46,48]. The figures also show sharp change of slope at about 25 min in the plots, demonstrating two distinct linear regions of adsorption, indicating existence of more than one type of diffusion process [29,44]. Furthermore, the agreement of experimental data with the PSO kinetic model suggests that chemisorption might dominate the adsorption process [28,49].

8. Challenges for commercial application of natural fiber–based ACF

8.1. Surface area vs. yield

Although ACFs have applications in a number of important areas such as ANG, gas separation, recovery of organic compounds and solvents, protective masks, treatment of air and wastewater, catalyst, refrigerator deodorizer, capacitors, etc., biomass-based ACFs have mostly been studied for treatment of wastewater and air. Very few studies dealing with gas storage have been reported so far [50]. The surface area of biomass-based ACF varies from 500 to 1,600 m^2/g in contrast with the surface area of synthetic ACF, such as those based on poly-acrylonitrile fiber, phenolic resin, pitch fiber, viscose fiber, etc., which varies

from 2,500 to 3,000 m^2/g [51–56]. High-end adsorbents used for applications such as ANG require high surface area, for example, 2,400 m^2/g, which is generally not met by biomass-based ACF. In one instance, bamboo fiber–based ACF was reported to attain surface area around 2,610 m^2/g, however, with very low yield.

8.2. Commercialization vs. use of chemicals

Commonly available commercial ACFs (either polymer or graphite based) provide surface area 1,000–1,800 m^2/g with a micro pore of 0.5–10 nm [57–59], which are well met by most of the reported cellulosic, that is, biomass-based ACF. However, biomass-based ACFs have not been very successful in meeting the industrial requirements to date for following reasons:

First, the biomass-based ACFs are reportedly fragile with very low tensile strength. ACFs synthesized from pitch, PAN or organic resin have tensile strength ranging from 70 to 500 MPa [5]. No study on biomass-based ACF has reported tensile strength of activated fibers. Fidelis et al. [60] measured the tensile strength of a 10–60 nm jute fiber, which varied from 250 to 324 MPa. After carbonization and activation, the strength of the fiber is expected to reduce significantly. Second, the ACFs made from natural fibers are non-uniform with discontinuous filament structure and low degree of orientation. They also possess impurities such as lignin and hemicellulose. Furthermore, due to variations in different batches of raw fibers, reproducing the properties of resultant activated fiber is sometimes difficult.

Researchers are trying to overcome the challenges in attaining large surface area with considerable yield and fiber strength, uniformity and reproducibility of fiber properties by treating the fibers with chemicals either before or during activation. The amount of chemicals being used is ranging from 1 to 10 kg chemicals per kg carbonized biomass. The washing of chemical impurities from activated fibers requires further use of chemicals or wash-water at least 100–500 times of the resultant ACF by weight. It is to be noted that biomass-based ACFs are preferred for its low cost and environment friendly application. Application of too many chemicals, including pollutants such as flame retardants, and use of wash water in large volume will increase the processing cost and water footprint of the ACF as well as health hazards.

Table 11
Kinetic parameters of the pseudo-first-order model obtained through non-linear regression

Dye	K_1	q_e	R^2
4-NP	0.088	36.59	0.966
MB	0.081	35.91	0.970

9. Conclusion and outlook

The literature review shows that jute fiber, coconut fiber, bamboo fiber, and waste cotton are some of the suitable ligno-cellulosic precursors for ACF production. For jute and cotton, the reported surface area varies between 450 and 900 m^2/g. The highest surface area ranging from 1,100 to 1,600 m^2/g is reported for coconut and bamboo fibers with an example of coconut fiber reaching as high as 2,169 m^2/g. The existing studies also recommend chemical pretreatment/activation over physical activation of biomass to get reasonable yield, surface area, inner porosity and fiber structure with lower temperature and shorter activation time. Studies on adsorption isotherms and adsorption kinetics of different dyes on ACF report that both Langmuir and Freundlich models are suitable for describing the isotherms while PSO kinetic model fits the adsorption rate data best.

The experimental work on ACF, prepared from jute fiber, conducted under present study shows that pretreatment of the raw material with flame retardants followed by chemical activation was required to attain reasonable surface area and pore volume of the resultant ACFs. Preparation conditions that produced ACF with best properties are pretreatment with DAP and chemical activation with 65% H_3PO_4 at 700°C for 30 min. The specific surface area of the resulting ACF reached 552 m^2/g with a yield of 29.3% and a pore volume of 0.42157 cm^3/g. The adsorption study of the prepared ACFs with methylene blue (MB) and 4-nitrophenol (4-NP) solutions shows that the adsorption isotherms best fitted the Langmuir model, while the adsorption kinetics were adequately described by the PSO model for both dyes. The non-linear regression of the PFO model gave a better fit to the experimental data than that of the linear regression. Additionally, adsorption capacity and adsorption rate of 4-NP were found higher than those of MB.

The global market for ACF in coming years is anticipated to increase due to increasing environmental concerns related to air and water pollution coupled with rising demand from the protective clothing industry and growing applications in natural gas and in storage of methane.

Table 12
Summary of experimental and calculated adsorption capacities in both mass basis and molar basis

Model name	4-NP		MB	
	q_e (mg/g)	q_e (mol/g) × 10^6	q_e (mg/g)	q_e (mol/g) × 10^6
PFO linear	18.6	133.7	20.3	63.5
PSO linear	41.0	294.7	40.9	127.9
PFO Non-linear	36.6	263.0	35.9	112.3
Experimental	39.9	286.8	39.0	121.9

PFO: pseudo-first-order; PSO: pseudo-second-order.

Besides, as the number of patients of chronic kidney diseases is on rise globally, the demand for ACF in the dialysis applications will also heighten. In all these applications, particularly, in medical purposes, use of natural fiber–based ACF is preferred over synthetic ones.

Thus, research on biomass-based ACF should be oriented towards the search of new biomass as well as modification of already studied biomass precursors to produce ACF with improved physical properties and suitable for diversified and specific applications. Previous research showed that well-controlled chemical activations can modify the development of porosity substantially and can help in achieving preferential pore size distribution in ACF. Research on biomass-based ACF to produce tailor made pore-distribution for particular and high-end products should be carried out.

Chemical treatment is found to be essential in manufacturing biomass-based ACF. However, low yield, low surface area, high energy requirement and cost of chemicals and processing may override the low cost and environment-friendly advantage of biomass-based ACF. Thus, research to minimize use of chemicals and maximize energy saving during activation and to find efficient procedure for washing without compromising the quality of ACF will be vital in coming days.

Finally, although a number of studies reported adsorption kinetics of biomass-based ACFs in batch processes, there is almost no study reporting adsorption in packed bed. It is important to study the breakthrough curves as well as regeneration efficiency and durability of biomass-based ACFs in packed bed for industrial and commercial use.

References

[1] M. Smisek, S. Cerney, Active Carbon: Manufacture, Properties and Applications, Elsevier, Amsterdam, 1970, pp. 286–290.
[2] T. Lee, C. Ooi, R. Othman, F. Yeoh, Activated carbon fiber - the hybrid of carbon fiber and activated carbon, Rev. Adv. Mater. Sci., 36 (2014) 118–136.
[3] X. Ge, Z. Wu, Y. Yan, G. Cravotto, B.C. Ye, Enhanced PAHs adsorption using iron-modified coal-based activated carbon via microwave radiation, J. Taiwan Inst. Chem. Eng., 64 (2016) 235–243.
[4] M.A. Yahya, Z. Al-Qodah, C.Z. Ngah, Agricultural bio-waste materials as potential sustainable precursors used for activated carbon production: a review, Renewable Sustainable Energy Rev., 46 (2015) 218–235.
[5] L. Zhang, L. Tu, Y. Liang, Q. Chen, Coconut-based activated carbon fibers for efficient adsorption of various organic dyes, RSC Adv., 8 (2018) 42280–42291.
[6] N.H. Phan, S. Rio, C. Faur, L. Le Coq, P. Le Cloirec, T.H. Nguyen, Production of fibrous activated carbons from natural cellulose (jute, coconut) fibers for water treatment applications, Carbon, 44 (2006) 2569–2577.
[7] V.K. Gupta, P.J.M. Carrott, R. Singh, M. Chaudhary, S. Kushwaha, Cellulose: a review as natural, modified and activated carbon adsorbent, Bioresour. Technol., 216 (2016) 1066–1076.
[8] A. Jain, R. Balasubramanian, M.P. Srinivasan, Hydrothermal conversion of biomass waste to activated carbon with high porosity: a review, Chem. Eng. J., 283 (2016) 789–805.
[9] H. Tounsadi, A. Khalidi, M. Abdennouri, N. Barka, Activated carbon from Diplotaxis Harra biomass: optimization of preparation conditions and heavy metal removal, J. Taiwan Inst. Chem. Eng., 59 (2016) 348–358.
[10] M. Asadullah, M.S. Kabir, M.B. Ahmed, N.A. Razak, N.S.A. Rasid, A. Aezzira, Role of microporosity and surface functionality of activated carbon in methylene blue dye from water, Korean J. Chem. Eng., 30 (2013) 2228–2234.
[11] A. Roy, S. Chakraborty, S.P. Kundu, R.K. Basak, S.B. Majumder, B. Adhikari, Improvement in mechanical properties of jute fibers through mild alkali treatment as demonstrated by utilization of the Weibull distribution model, Bioresour. Technol., 107 (2012) 222–228.
[12] S. Senthilkumaar, P.R. Varadarajan, K. Porkodi, C.V. Subbhuraam, Adsorption of methylene blue onto jute fiber carbon: kinetics and equilibrium studies, J. Colloid Interface Sci., 284 (2005) 78–82.
[13] P.T. Williams, A.R. Reed, Development of activated carbon pore structure via physical and chemical activation of biomass fiber waste, Biomass Bioenergy, 30 (2006) 144–152.
[14] H. Ku, H. Wang, N. Pattarachaiyakoop, M. Trada, A review on the tensile properties of natural fiber reinforced polymer composites, Composites B, 42 (2011) 856–873.
[15] M. Ramesh, K. Palanikumar, K. Hemachandra Reddy, Mechanical property evaluation of sisal–jute–glass fiber reinforced, Composites B, 48 (2013) 1–9.
[16] A. Dąbrowski, Adsorption and Its Applications in Industry and Environmental Protection, Elsevier, Amsterdam, 1999, pp. 69–94.
[17] J.Y. Chen, Activated Carbon Fiber and Textiles, Woodhead Publishing, Cambridge, 2017, pp. 22–71.
[18] M.M. Tang, R. Bacon, Carbonization of cellulose fibers. 1. Low temperature pyrolysis, Carbon, 2 (1964) 211–214.
[19] M.A. Tadda, A. Ahsan, A. Shitu, M. Elsergany, T. Arunkumar, B. Jose, N.N. Nik, A review on activated carbon: process, application and prospects, J. Adv. Civ. Eng. Pract. Res., 2 (2016) 7–13.
[20] C.F.S. Rombaldo, A.C.L. Lisboa, M.O.A. Mendez, A.R. Coutinho, Brazilian natural fiber (jute) as raw material for activated carbon production, An. Acad. Bras. Cienc., 86 (2014) 2137–2144.
[21] X. Zhou, S.H. Ghaffar, W. Dong, O. Oladiran, M. Fan, Fracture and impact properties of short discrete jute fibre-reinforced cementitious composites, Mater. Des., 49 (2013) 35–47.
[22] A. Bledzki, J. Gassan, Composites reinforced with cellulose based fibres, Prog. Polym. Sci, 24 (1999) 221–274.
[23] J. Rosas, J. Bedia, J. Rodríguez-Mirasol, T. Cordero, Hemp-derived activated carbon fibers by chemical activation with phosphoric acid, Fuel, 88 (2009) 19–26.
[24] Y. Zhao, F. Fang, H.M. Xiao, Q.P. Feng, L.Y. Xiong, S.Y. Fu, Preparation of pore-size controllable activated carbon fibers from bamboo fibers with superior performance for xenon storage, Chem. Eng. J., 270 (2015) 528–534.
[25] K. Hina, H. Zou, W. Qian, D. Zuo, C. Yi, Preparation and performance comparison of cellulose-based activated carbon fibres, Cellulose, 25 (2017) 607–617.
[26] K.L. Chiu, D.H.L. Ng, Synthesis and characterization of cotton-made activated carbon fiber and its adsorption of methylene blue in water treatment, Biomass Bioenergy, 46 (2012) 102–110.
[27] E. Ekrami, F. Dadashian, M. Soleimani, Waste cotton fibers based activated carbon: optimization of process and product characterization, Fibers Polym., 15 (2014) 1855–1864.
[28] T.L. Silva, A.L. Cazetta, P.S.C. Souza, T. Zhang, T. Asefa, V.C. Almeida, Mesoporous activated carbon fibers synthesized from denim fabric waste: efficient adsorbents for removal of textile dye from aqueous solutions, J. Cleaner Prod., 171 (2018) 482–490.
[29] K.K. Beltrame, A.L. Cazetta, P.S.C. de Souza, L. Spessato, T.L. Silva, V.C. Almeida, Adsorption of caffeine on mesoporous activated carbon fibers prepared from pineapple plant leaves, Ecotoxicol. Environ. Saf., 147 (2018) 64–71.
[30] X. Ma, F. Zhang, J. Zhu, L. Yu, X. Liu, Preparation of highly developed mesoporous activated carbon fiber from liquefied wood using wood charcoal as additive and its adsorption of methylene blue from solution, Bioresour. Technol., 164 (2014) 1–6.
[31] A. Vargas, A.L. Cazetta, M. Kunita, T. Silva, V. Almeida, Adsorption of methylene blue on activated carbon produced from flamboyant pods (*Delonix regia*): study of adsorption isotherms and kinetic models, Chem. Eng. J., 168 (2011) 722–730.
[32] S. Ltenor, B. Carene, E. Emmanuel, J. Lambert, J. Ehrhardt, S. Gaspard, Adsorption studies of methylene blue and phenol

onto vetiver roots activated carbon prepared by chemical activation, J. Hazard. Mater., 165 (2008) 1029–1039.
[33] F. Avelar, M. Bianchi, M. Goncalves, E. Mota, The use of Piassava fibers (*Attalea funifera*) in the preparation of activated carbon, Bioresour. Technol., 101 (2010) 4639–4645.
[34] C.U. Pittman, W. Jiang, Z.R. Yue, S. Gardner, L. Wang, H. Toghiani, C.A. Leon y Leon, Surface properties of electrochemically oxidized carbon fibers, Carbon, 37 (1999) 1797–1807.
[35] C.U. Pittman, W. Jiang, Z.R. Yue, C.A. Leon y Leon, Surface area and pore size distribution of microporous carbon fibers prepared by electrochemical oxidation, Carbon, 37 (1999) 85–96.
[36] L.G. Tang, J.L. Kardos, A review of methods for improving the interfacial adhesion between carbon fiber and polymer matrix, Polym. Compos., 18 (1997) 100–113.
[37] Z.R. Yue, W. Jiang, L. Wang, S.D. Gardner, C.U. Pittman, Surface characterization of electrochemically oxidized carbon fibers, Carbon, 37 (1999) 1785–1796.
[38] Z.R. Yue, W. Jiang, L. Wang, H. Toghiani, S.D. Gardner, C.U. Pittman, Adsorption of precious metal ions onto electrochemically oxidized carbon fibers, Carbon, 37 (1999) 1607–1618.
[39] J.C. Chen, I.R. Harrison, Modification of polyacrylonitrile (PAN) carbon fiber precursor via post-spinning plasticization and stretching in dimethyl formamide (DMF), Carbon, 40 (2002) 25–45.
[40] M.S.A. Rahaman, A.F. Ismail, A. Mustafa, A review of heat treatment on polyacrylonitrile fiber, Polym. Degrad. Stab., 92 (2007) 1421.
[41] S. Mopoung, P. Amornsakchai, S. Somroop, Characterization of phosphoric acid modified activated carbon fiber from fiber waste of pineapple leaf fiber production processing, Carbon Sci. Technol., 8 (2016) 1–12.
[42] C.-I. Su, R.-S. Yeh, C.-L. Wang, Influence of flame retardant on manufacturing carbon fiber absorbents, Text. Res. J., 74 (2004) 966–969.
[43] C.-I. Su, C.-L. Wang, Optimum manufacturing conditions of activated carbon fiber absorbents. I. Effect of flame-retardant reagent concentration, Fibers Polym., 8 (2007) 477–481.
[44] X. Duan, C. Srinivasakannan, X. Wang, F. Wang, X. Liu, Synthesis of activated carbon fibers from cotton by microwave induced H_3PO_4 activation, J. Taiwan Inst. Chem. Eng., 70 (2017) 374–381.
[45] K.Y. Foo, B.H. Hameed, Microwave-assisted preparation of oil palm fiber activated carbon for methylene blue adsorption, Chem. Eng. J., 166 (2011) 792–795.
[46] R. Ma, X. Qin, Z. Liu, Y. Fu, Adsorption property, kinetic and equilibrium studies of activated carbon fiber prepared from liquefied wood by $ZnCl_2$ activation, Materials, 12 (2019) 1377.
[47] S. Zamani, N.S. Tabrizi, Removal of methylene blue from water by graphene oxide aerogel: thermodynamic, kinetic, and equilibrium modeling, Res. Chem. Intermed., 41 (2014) 7945–7963.
[48] H. Al-Aoh, R. Yahya, M.J. Maah, M.R. Bin Abas, Adsorption of methylene blue on activated carbon fiber prepared from coconut husk: isotherm, kinetics and thermodynamics studies, Desal. Water Treat., 52 (2013) 6720–6732.
[49] C. Djilani, R. Zaghdoudi, F. Djazi, B. Bouchekima, A. Lallam, A. Modarressi, M. Rogalski, Adsorption of dyes on activated carbon prepared from apricot stones and commercial activated carbon, J. Taiwan Inst. Chem. Eng., 53 (2015) 112–121.
[50] H. Marsh, D.C. Crawford, T.M. O'Grady, A. Wennerberg, Carbons of high surface area. A study by adsorption and high-resolution electron microscopy, Carbon, 20 (1982) 419–426.
[51] J. Maciá-Agulló, B.C. Moore, D. Cazorla-Amorós, A. Linares-Solano, Activation of coal tar pitch carbon fibres: physical activation vs. chemical activation, Carbon, 42 (2004) 1367–1370.
[52] H. Marsh, D.A. Taylor, J.R. Lander, Kinetic study of gasification by oxygen and carbon dioxide of pure and doped graphitizable carbons of increasing heat treatment temperature, Carbon, 19 (1981) 375–381.
[53] M.A. Daley, C.L. Mangun, J.A. DeBarrb, S. Riha, A.A. Lizzio, G.L. Donnals, J. Economy, Adsorption of SO_2 onto oxidized and heat-treated activated carbon fibers (ACFS), Carbon, 35 (1997) 411–417.
[54] A. Oya, S. Yoshida, J. Alcañiz-Monge, A. Linares-Solano, Formation of mesopores in phenolic resin-derived carbon fiber by catalytic activation using cobalt, Carbon, 33 (1995) 1085–1090.
[55] D. Das, V. Gaur, N. Verma, Removal of volatile organic compound by activated carbon fiber, Carbon, 42 (2004) 2949–2962.
[56] M. Suzuki, Activated carbon fiber: fundamentals and applications, Carbon, 32 (1994) 577–586.
[57] UNITIKA, Activated Carbon Fibers. Available at: https://www.unitika.co.jp/acf/e/products/a-carbon-fibers/ (Accessed on March 28, 2020).
[58] HP Materials Solutions Inc., Activated Carbon Fiber & Activated Carbon Felt. Available at: https://www.hpmsgraphite.com/activatedcarbonfiber.html (Accessed on March 27, 2020).
[59] TOYOBO Co. Ltd., K-Filter (The Activated Carbon Fiber). Available at: https://www.toyobo-global.com/seihin/ac/filter/k-filter/#type (Accessed on March 28, 2020).
[60] M.E.A. Fidelis, T.V.C. Pereira, O.D.F.M. Gomes, F. De Andrade Silva, R.D. Toledo Filho, The effect of fiber morphology on the tensile strength of natural fibers, J. Mater. Res. Technol., 2 (2013) 149–157.